ANALYSIS OF IN-FLIGHT MEASUREMENTS FROM HELICOPTER TRANSMISSIONS

Marianne Mosher and Edward M. Huff
Computational Sciences Division
NASA Ames Research Center

Eric Barszcz
QSS Group, Inc.
NASA Ames Research Center

ABSTRACT

In-flight vibration measurements from the transmission of an OH-58C KIOWA are analyzed. In order to understand the effect of normal flight variation on signal shape, the first gear mesh components of the planetary gear system and bevel gear are studied in detail. Systematic patterns occur in the amplitude and phase of these signal components with implications for making time synchronous averages and interpreting gear metrics in flight. The phase of the signal component increases as the torque increases; limits on the torque range included in a time synchronous average may now be selected to correspond to phase change limits on the underlying signal. For some sensors and components, an increase in phase variation and/or abrupt change in the slope of the phase dependence on torque are observed in regions of very low amplitude of the signal component. A physical mechanism for this deviation is postulated. Time synchronous averages should not be constructed in torque regions with wide phase variation.

INTRODUCTION

The analysis of transmission vibration is an important aspect of modern helicopter Health Usage and Monitoring Systems (HUMS). It is generally hoped that flight safety can be improved, and maintenance costs reduced, by identifying characteristic damage patterns well in advance of in-flight failures. The detection of faults in flight is still a developing area with [1] finding the need for the improvement of diagnostic performance. The authors of this paper believe the dynamic flight environment is a major source of difficulty in the diagnostic performance. Current diagnostic methods were not found to detect a serious crack in the planetary gear system of the UH-60A in flight [2].

This study is part of a continuing program at NASA Ames Research Center into the research of flight effects on fault detection in rotating machinery [3-8]. Past studies have shown significant dependence of vibration signal amplitude upon torque [3, 4, 7] and dependence of the signal amplitude upon flight maneuver [3-6]. A new aspect of this study is the use of measurements made in free flight instead of prescribed maneuvers. The addition of GPS measurements brings more flight state parameters into the study of vibration on the OH-58C in flight. Also, shaft revolution counting is added to allow tracking of the shaft position for all the gear shafts. Thus comparisons can be made between time histories for gears on any shaft from data records acquired in the same flight.

Many of the metrics developed to detect damage in gears, such as FM4, N6A, N8A, N4A, NB4, energy ratio and sideband level factor, are based upon characteristics of the shape of the signal, as opposed to the amplitude of the vibration signal. Good descriptions of these metrics are summarized in [9, 10]. This paper introduces the study of the basic signal shape as a function of the flight state space.

This work examines vibrations measured in flight of the OH-58C Kiowa at NASA Ames Research Center. The hardware and experiment will be described. Analysis includes examination of the signal component shapes in the time domain.

OBJECTIVES

The objective of this research is to further the understanding of the vibration from transmissions in aircraft during flight. The increased understanding can then be applied to improve fault detection and reduce false alarms in the dynamic flight environment.

Presented at the American Helicopter Society 60th Annual Forum, Baltimore, MD, June 7-10, 2004.

DATA COLLECTION

Transmission Description

The OH-58C is a light weight helicopter (Figure 1). The main transmission on the OH-58C Kiowa contains two reduction stages. A 19-tooth pinion on the output shaft of the engine meshes with a 71-tooth spiral bevel gear to provide the first stage. An epicyclic gearbox with fixed ring gear provides the second reduction stage. The sun gear is on the shaft containing the spiral bevel gear from the first stage. The planetary gear system contains 99 teeth on the ring gear, 27 teeth on the sun gear and 35 teeth on the planet gears. This helicopter model contains four planet gears in two pairs of two gears; each gear pair is spaced 180 deg with about 91.4 deg between the pairs. The planet carrier section of the epicyclic system, in turn, drives the main rotor. The turbine engine powering the helicopter contains an output gearbox with extensive gearing to provide much of the necessary speed reduction prior to entering the transmission. A 50-tooth gear on the output of the turbine gearbox is on the other end of the shaft that drives the pinion in the transmission. Since the 50-tooth gear is rotating at exactly the same speed as the pinion, it must be considered when testing the 19-tooth pinion gear.

Figure 1 OH58-C Kiowa

Sensors

Measurements of transmission vibration, torque, main rotor rotational speed (RPM), and aircraft position and velocity relative to the ground were made on an OH-58C Kiowa in flight. Vibration measurements were taken with three uni-axial and one tri-axial accelerometers mounted on vertical bolts on the transmission housing. Accelerometers 1, 2 and 3 were horizontal and oriented radial to the transmission at 129 deg, 206 deg and 309 deg from the pinion shaft. Accelerometers 4, 5 and 6 were on the tri-axial mount at 51 deg from the pinion shaft with number 4 tangential to the transmission, number 5 vertical to the transmission housing and number 6 horizontal and radial to the transmission housing. Torque was derived from engine oil pressure. Rotational speed was derived from a tachometer pulse originating on the main rotor shaft. These six channels of vibration measurements along with engine torque and the once-per-rotation tachometer pulse signal were digitized and stored on a PC based data acquisition system that is part of Healthwatch-2. All signals were digitized to 12 bits at 50 kHz per channel after an 18 kHz low pass anti-aliasing filter. Gains were set to maximize the signal in the digitizing range while minimizing clipping. Helicopter position and velocity with respect to the ground are measured with GPS. Barszcz [11] contains more information on the Healthwatch-2 data acquisition system.

Calibration

For the accelerometers, sensitivity of the accelerometer (provided by the manufacturer) and a resister value determine the conversion from voltage to acceleration. The expected accuracy is about 5%. No attempt was made to track drift. Tap tests were performed on the mounted accelerometers to look for resonances. Measurements were made of about 10 averages in the frequency domain of the accelerometer power spectrum, hammer power spectrum, frequency response function from hammer to accelerometer and the coherence between the two signals. Five accelerometers tested show multiple peaks in the frequency response; all above 5 kHz (accelerometer #1 was not available at the time of testing). Since the current analysis is confined to the first gear mesh component, all analyses are done at frequencies below the peaks revealed in the tap test. Also, the resonances found in the tap test are not so large as to interfere with analysis at and near the frequencies of the gear components.

The torque measurement was calibrated by applying pressure to the oil line, reading the torque off the aircraft display on the aircraft and measuring through the data acquisition system. Several readings were taken as the pressure was first increased from 0 to 75 psi and then reduced back to 0. Since levels were stabilized before reading, this calibration is a static calibration. No dynamic characteristics were measured. Details of the torque calibration are presented in [11].

Table 1 OH-58C Transmission

Gear	Teeth	Shaft ratio	Gear mesh, rotor shaft orders	Gear mesh frequency Hz at 360 rpm of main rotor
Planetary				
Ring	99		99	594
Planet	35		99	594
Sun	27		99	594
Carrier		1		
Bevel	71	(99+27)/27 = 4.6667	331.3333	2772
Pinion	19	(71/19)*(99+27)/27 = 17.4386	331.3333	2772
Turbine	50	(71/19)*(99+27)/27 = 17.4386	871.9298	7295

Flight Process

This paper presents results from eight flights of the OH-58C acquired in October, November and December of 2003 at NASA Ames Research Center. All 740 34-second data records were collected on a free flight basis, in which the system collects, processes and stores data then immediately collects the next data record. The pilot turned the data acquisition system on at the beginning of the flight, off at the end of the flight, and did not initiate collection of individual data records. The flight conditions of individual records were not controlled in this set of flights as they had been in previous flights [2, 3]. The pilot flew a standardized mission, Table 2, for the first five flights (516 data records), and training flights with more variable flight conditions for the last three flights (224 data records).

Table 2 Mission Description for Flights 1 – 5.

Pressure Altitude, ft	Target Speed, Kt	Flight Condition
3500	100	Cruise
3500	75	Cruise
3500	45	Cruise
3500 to 9500	45	Climb at 100 fpm
9500	45	Cruise
9500	60	Cruise
9500	75	Cruise
9500 to 8500	75	Descend at 500 fpm
8500	85	Cruise
8500	65	Cruise
8500	45	Cruise
8500 to 2500	45	Descend 1000 fpm
2500	45	Cruise
2500	65	Cruise
2500	85	Cruse
2500 to 1000	100	Descend 500 fpm
1000	100	Transition

Figure 2 and 3 show distributions of RPM and torque for the first five and the last three flights respectively. Each rectangle represents a bin colored by the number of data points falling within the bin, darker rectangles contain more data. Note that most data fall in the range 40% to 80% torque and 356 to 362 RPM, with some data ranging out in all directions. The increase in RPM for lower torque can be seen in these figures. The discrete mission flight conditions produce a few dense clusters in the torque-RPM plane. Note that although most of the flight conditions fall in a band containing these clusters, some instances fall far outside this band in torque-RPM space.

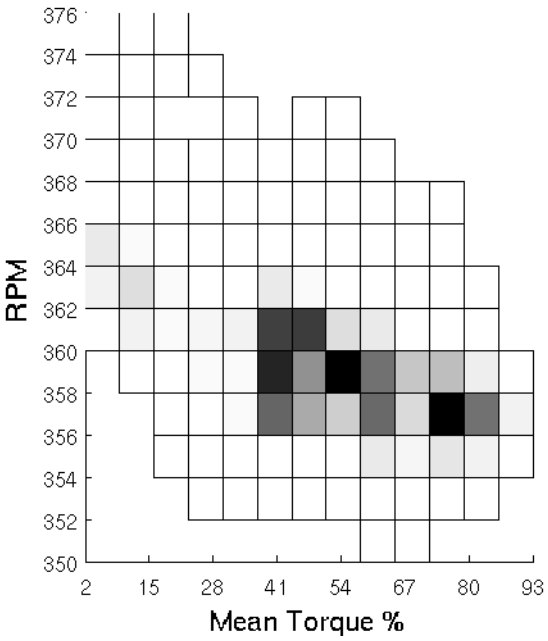

Figure 2 Distribution of Torque and RPM for 5 flights with standardized mission.

Presented at the American Helicopter Society 60th Annual Forum, Baltimore, MD, June 7-10, 2004.

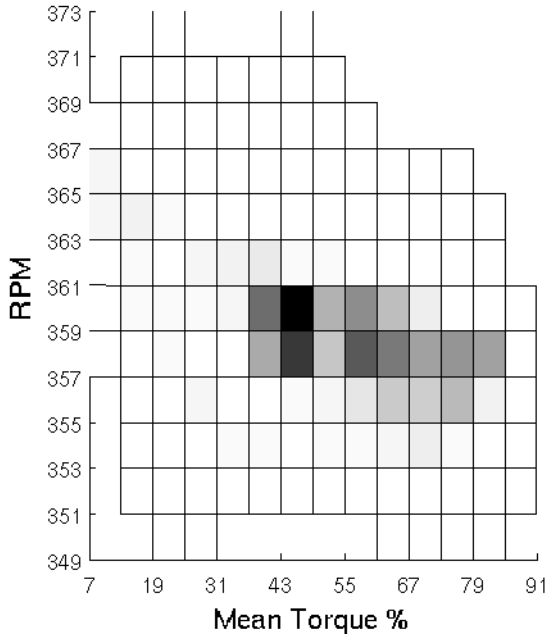

Figure 3 Distribution of Torque and RPM for 3 training flights.

Signal Quality

Various data quality checks were performed on the archived flight data. File integrity checks involve examining the size of the file and computing checksums. Each file has an internal header that contains information about the contents of the file. Header values such as the main rotor revolution count are checked for consistency across the entire flight. Other header fields are used to compute the amount of data that should be present and compared against the actual amount.

Integrity checks of the sampled signals vary with the type of data collected over the channel. No tests are performed on the torque data. For the tachometer channel, revolution boundaries are determined and the number of revolutions computed. This number is compared against the values of the revolution counter, recorded at the start and end of each sampling period and stored in the header. In addition, the duration of each revolution is computed and any outliers flagged.

For vibration data channels, the number and size of clipped regions are counted. A point is clipped if it has a value of either +2047 or -2048 for 12-bit data. The size of a region is determined by the number of successive points that are clipped. In addition to clipped regions, plateau regions are counted. Similar to a clipping region a plateau region is where two or more successive samples have identical values, excluding +2047 and -2048. Plateaus exceeding four points long are considered suspicious.

DATA ANALYSIS

Flight State Space

For this research, flight state parameters were processed outside of Healthwatch-2 in order to include measures from the GPS system. The measurements relating to the state of the aircraft available in these flights are the torque of the transmission, the rotational speed of the main rotor (RPM), the latitude, longitude, height above sea level, vertical velocity (rate of climb, ROC), ground velocity east, ground velocity north and number of main rotor rotations from the start of the data collection program. All parameters were processed to yield one datum per each main rotor rotation. Torque was collected through the 50 kHz digitizer and processed into mean torque, variance of torque and central difference of torque. RPM was derived from the tachometer signal. The position and velocity information were collected through the GPS, time tracked by the main rotor revolution count (from the tachometer) and interpolated to give one value per rotation of the main rotor. The ground speed was derived from the north and east velocities. Air speed is preferred to ground speed, but was not derivable from the available measurements. The number of rotations from the start is a variable related to the gross weight: as the flight progresses the rotation number increases and the weight decreases. The relationship between gross weight and rotation count is not exactly linear due to changes in fuel consumption with changes in the flight condition. The gross weight is preferred, but not available.

Preprocessing to Construct Averages

For analysis of the components of the transmission, the vibration samples are resampled from a time base to a gear shaft revolution base and averaged. The resampling is done with a cubic spline using the tachometer pulse signal as reference and placing sampling locations evenly between the pulses. For the planetary gear, 8192 samples are used in each rotation of the carrier. For the bevel gear, 2048 samples are used for each rotation of its shaft. All of these resamplings conform to the Nyquist criteria without additional filtering.

Averages were constructed with the Healthwatch-2 system [11] operating in the off-line mode. Time synchronous averages were constructed for the various gears. With time synchronous averaging, noise and discrete frequency signals not commensurate with the

block size are reduced in amplitude so the periodic components of the signal are emphasized. Averages contain 99 carrier rotations for the planetary gear and 19 rotations for the bevel. The number of epochs used is based upon three criteria, noise reduction, stationarity and gear meshing cycles with mating gears. These criteria are discussed in [6], particularly with respect to the pinion gear on the OH-58C. The number of epochs chosen meets all three criteria for the bevel gear. The number of epochs chosen for the planetary gear only meets the noise reduction and mating gear meshing criteria; the number of epochs is too large for providing good stationarity; yet, for much of the data, the long time sample is not far from stationary.

The time synchronous averages from the tri-axial accelerometer were rotated based upon principle component analysis similar to the analysis by Tumer [5]. For these data, a rotation matrix was constructed separately for each of the gears, carrier and bevel, and applied to each separately. Each rotation matrix came from the covariance matrix of the gears time synchronous average for the entire eight flights. These rotated signals will be referred to as PC1, PC2 and PC3.

Amplitude and Phase of First Gear Mesh Component

The amplitude and phase of the first gear mesh component are simple parameters relating to the shape of the vibration signal. By studying these, we can start to understand the effects of flight state upon the shape of the vibration signal. Processing of the planetary gear system is described, followed by processing of the bevel gear.

The planetary gear system generates vibrations with a complicated spectrum when measured at a sensor fixed on the transmission housing and not rotating with the planet gears. References [12-14] contain descriptions of this complicated signal. Reference [14] describes the model that is used here to isolate the vibration signal associated with the first gear mesh harmonic of the planetary gear system.

To derive an amplitude and phase associated with the first gear mesh harmonic, first the analytic signal containing the frequency components near the gear mesh frequency that contribute to the idealized planetary signal is constructed. The analytic signal is the analytic continuation of the real signal; the analytic signal is a complex valued vector in which the real part is the vibration signal and the imaginary part is the Hilbert transform of the vibration signal. For the OH58C, this analytic signal contains the even harmonics of the carrier shaft orders from 78 through 116. Figure 4 shows a sample time synchronous average and filtered vibration signal. The analytic signal has the appearance of an oscillatory signal with both amplitude and frequency variation. In general, these can be viewed as the amplitude increasing as a planet gear is closest to the sensor and the frequency varying as a result of changing interference among the vibration from all the planet gears. Changing interference among the vibration signals from all the planet gears also contributes to the amplitude variation.

The amplitude of the first gear mesh component is evaluated as the root mean square of the filtered vibration signal containing the even harmonics of the carrier shaft orders from 78 through 116. The phase of the first gear mesh component is evaluated at a fixed time index in the carrier shaft rotation corresponding to the maximum of the average of the amplitude of the analytic signals over all flights. By picking the location of the maximum of the average analytic signal (see vertical line in Figure 4), this location is expected to be at or near the passage of a planet gear by the sensor. If an arbitrary index, such as the first time step, were used, the amplitude of the signal could be very low contributing to a noisier phase measurement.

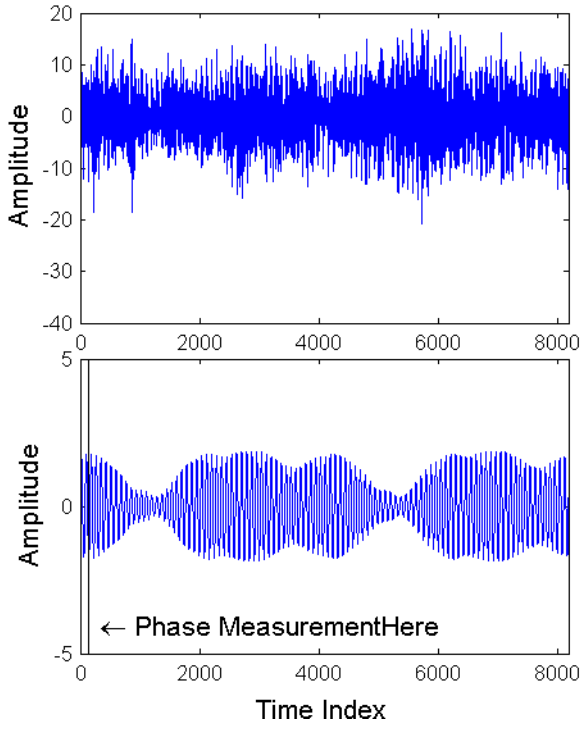

Figure 4 Planetary System Vibration, a) Time Synchronous Average, b) Time Synchronous Average of selected frequencies around gear mesh frequency.

For the bevel gear, only the single frequency component of 71 times the bevel shaft frequency is used to compute the amplitude and phase of the first gear shaft harmonic. The first gear mesh amplitude is the amplitude of the bevel gear mesh frequency in the spectrum. The phase of the gear mesh frequency is the phase of the analytic signal at the first time index in the time synchronous average. Figure 5 shows a sample time synchronous average and filtered vibration signal for the bevel gear.

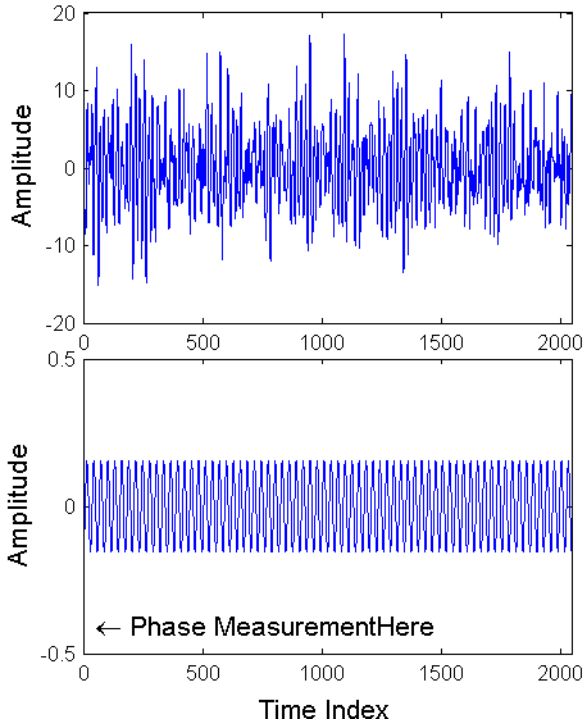

Figure 5 Bevel Gear Vibration, a) Time Synchronous Average, b) Time Synchronous Average gear mesh frequency.

RESULTS

Signal Quality

A small amount of clipping occurred, mostly on accelerometer 4. Table 3 lists the fraction of data points clipped; the columns group clippings by how many consecutive data points are clipped. A small number of plateaus occurred. Table 4 lists the fraction of data points with plateaus. The plateaus are not extensive enough to indicate open or short circuit problems.

Table 3 Fraction of Data Points Clipped

	1 clip	2 clip	3 clip	> 3 clip
Accel 1	0.000E+00	7.003E-10	0.000E+00	0.000E+00
Accel 2	1.401E-09	0.000E+00	0.000E+00	0.000E+00
Accel 3	0.000E+00	0.000E+00	0.000E+00	0.000E+00
Accel 4	2.526E-04	7.594E-05	1.315E-06	0.000E+00
Accel 5	0.000E+00	0.000E+00	0.000E+00	0.000E+00
Accel 6	2.941E-08	1.401E-09	0.000E+00	0.000E+00

Table 4 Fraction of Data Points with Plateaus

	4 consecutive points	5 consecutive points	>5 consecutive points
Accel 1	1.996E-07	2.101E-09	0.000E+00
Accel 2	1.555E-07	2.101E-09	0.000E+00
Accel 3	8.333E-08	7.003E-10	0.000E+00
Accel 4	2.101E-09	0.000E+00	0.000E+00
Accel 5	1.646E-07	2.101E-09	0.000E+00
Accel 6	9.104E-09	0.000E+00	0.000E+00

Flight State Space

The flight parameters are assumed to have a relationship with the vibration. The measured flight parameters also have some relationship to each other. The correlation coefficients among the parameters (Table 5) give an indication of the linear relationship among the parameters. Other aspects of the relationships can be gleaned from the scatter plots in Figure 6. The main diagonal subplots in Figure 6 contain histograms of the flight parameters. Even though revolution count has low correlation with other flight parameters (Table 5), the other flight parameters have very systematic changes with revolution count because of the mission profile.

Table 5 Correlation Coefficients among measured Parameters found to be important in modeling amplitude of gear signal components.

	Torque	RPM	Height	Rev Count	Ground Speed	ROC
Torque	1.000	-0.619	-0.262	-0.055	0.426	0.593
RPM	-0.619	1.000	0.498	-0.027	0.096	-0.535
Height	-0.262	0.498	1.000	-0.259	0.101	0.030
Rev	-0.055	-0.027	-0.259	1.000	-0.005	-0.269
Speed	0.426	0.096	0.101	-0.005	1.000	0.004
ROC	0.593	-0.535	0.030	-0.269	0.004	1.000

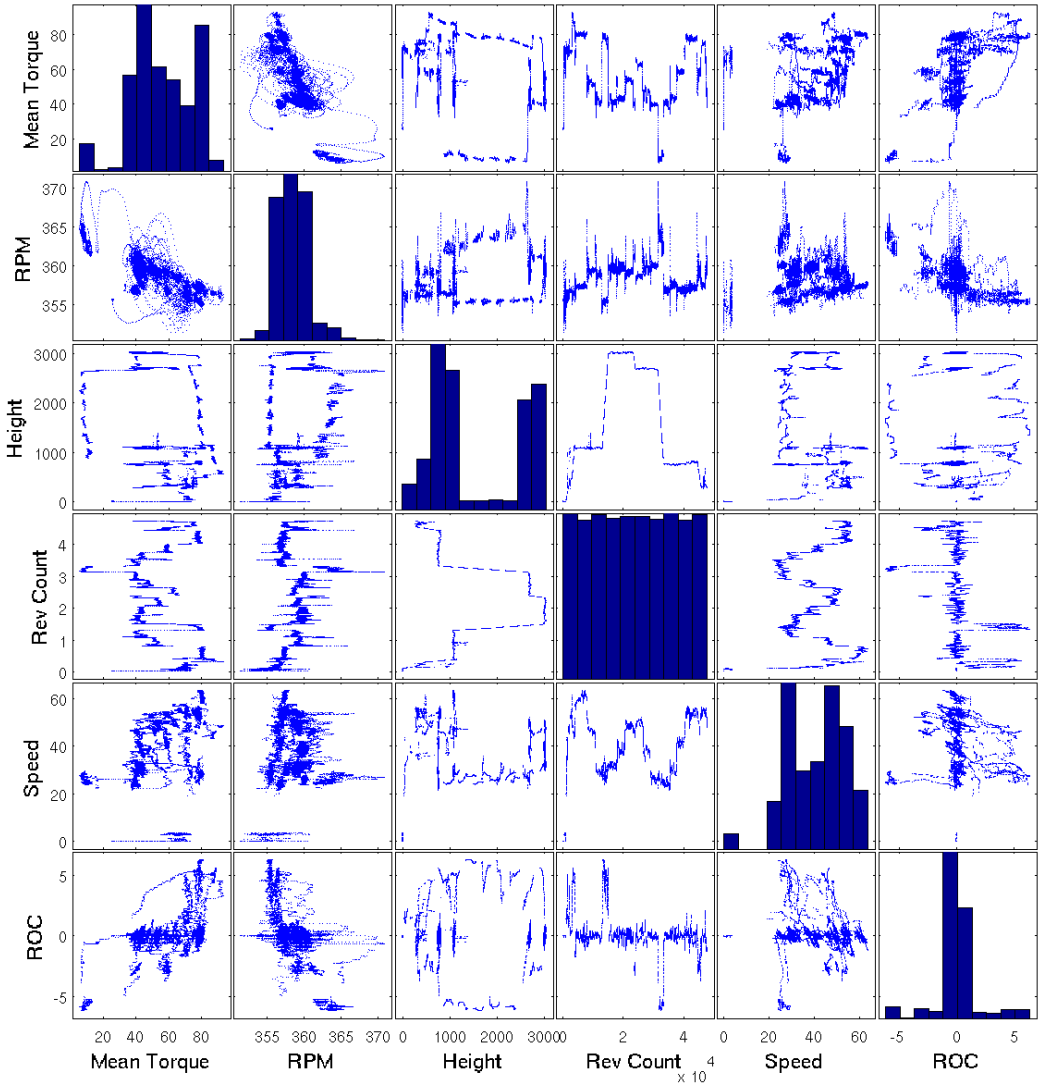

Figure 6 Scatter plot of selected flight parameters for the first flight.

Amplitude and Phase of First Gear Mesh Component

Planetary Gear System

The amplitude and phase of the first gear mesh component of the various gears all show a very strong functional dependence upon torque. Although the vibration signal of the first gear mesh component of the planetary gear system is more complex with more components, the dependence of its amplitude and phase upon the flight state is simpler than for the other gear studied. First, findings for the planetary gear system will be shown.

The amplitude of the first gear mesh component of the planetary system increases with torque, for all eight flights and six accelerometers. The first gear mesh component amplitude from accelerometers 1, 3 and 4 and the PC1 and PC3 display a highly linear dependence upon torque as can be seen in upper plot in Figure 7. The amplitude dependence on torque on the other channels, accelerometers 2, 5 and 6 and PC 2,

contains curvature as can be seen in the upper plot of Figure 8. Note the amplitude has a greater spread in the mid-torque range. This will be discussed in greater detail with data from the bevel gear.

The phase of the first gear mesh component of the planetary system increases with torque, for all eight flights and six accelerometers. The reference time for the average is the pulse from the magnetic pickup at the rotor head. The rotor mast extends between this once-per-rotation pulse generator and the planetary gear system. As torque is applied to the system, the shaft connecting the rotor head to the carriage on the planetary gear system can be expected to experience tortional strain. An increase in phase at the planetary gear relative to the rotor head is consistent with tortional strain in the mast as the torque from the engine is transferred through the planetary gear before the rotor. The relationship of phase to torque looks quite linear (lower plots in Figure 7 and Figure 8) with some curvature on some channels.

To examine the relationships in greater detail, linear regressions of phase on torque and amplitude on torque were made for the signals on all six accelerometers and all three rotated signals across all flights. The slopes and the correlation coefficients are shown for all these regressions in Table 6. Note that all the correlations are high, especially for the phase.

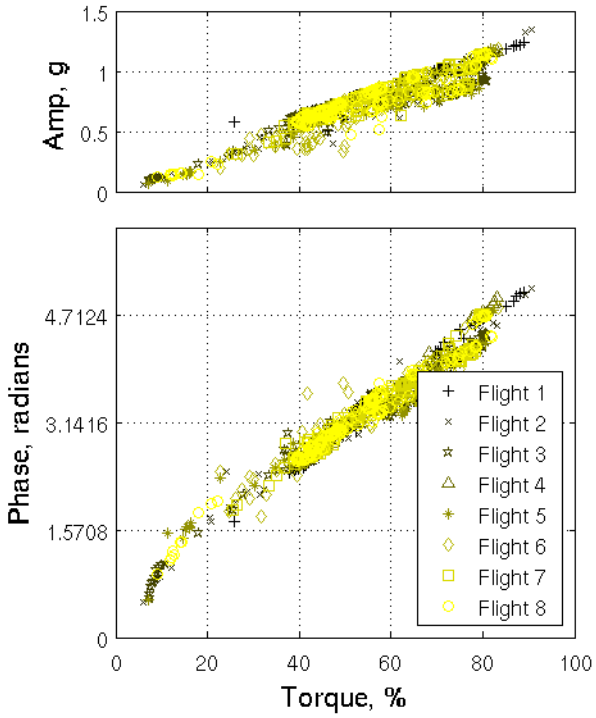

Figure 7 Measures of Planetary System First Gear Mesh Harmonic for Accelerator 1.

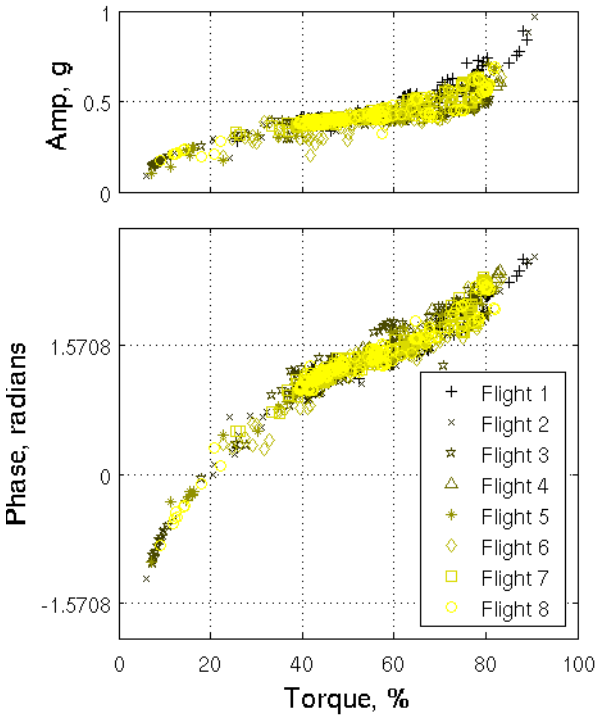

Figure 8 Measures of Planetary System First Gear Mesh Harmonic for Accelerator 2.

Table 6 Properties of Planetary System First Gear Mesh Harmonic Dependant upon Torque.

	Slope, Amplitude	Correlation, Amplitude	Slope, Phase	Correlation, Phase
Accel 1	0.0123	0.9308	0.0476	0.9817
Accel 2	0.0051	0.881	0.0314	0.9421
Accel 3	0.0175	0.9469	0.0492	0.9802
Accel 4	0.0059	0.8979	0.0488	0.9804
Accel 5	0.0077	0.8492	0.0262	0.9536
Accel 6	0.0075	0.9146	0.031	0.9699
PC 1	0.0078	0.9312	0.0471	0.9799
PC 2	0.0082	0.8637	0.0284	0.9614
PC 3	0.0048	0.8426	0.038	0.9743

Bevel Gear

The relationship of amplitude and phase of the first gear mesh harmonic of the bevel gear is more complicated than for the first gear mesh component of the planetary gear system.

The amplitude of the bevel gear mesh frequency component increases sharply at the lower torque levels below about 15% for all eight flights and all 6 accelerometers. Above about 20% torque the amplitude decreases then increases. A local maximum in gear mesh harmonic amplitude exists in the 15% to 20% torque range for all accelerometers and flights. The location, depth and steepness of the local minima vary among the signals from the six accelerometers. For accelerometer number 1, the local minimum is broad and located around 60 through 80 % torque, see upper plot in Figure 9. Local minima on the other accelerometers are more pronounced. On accelerometer number 3, the minimum is near 43% torque (upper plot Figure 10); on accelerometer number 4, the minimum is near 41% torque (upper plot in Figure 11); and on accelerometer number 5, the minimum is near 35% torque (upper plot in Figure 12). In all cases, the amplitude between about 60% and 80% torque shows a larger range; the amplitude data appears to be split between an upper and lower range in the 60% to 80% torque region.

The relationship between the phase of the bevel gear mesh frequency and torque is even more complex. In general, the phase increases as torque increases with a steeper slope than for the first gear mesh component of the planetary gear. Several systematic deviations from the general upward trend occur. For all signals, in the torque region of about 45% to 80%, the phase values have a broader range and appear to split into two regions as with the planetary gear. For all of the accelerometers except the first, there is a torque range with either flat or steeper phase at the same location as the local minima in amplitude. The general upward trend of phase with torque has about the same slope above and below the torque range with flat or steeper phase. When examined in some detail, the difference between the two generally linear parts of the torque-phase curve is about a jump of about π radians.

The jump in the phase curve is believed to be due to a change in the vibrational response of the structure resulting in the accelerometer being on one side of a node below the jump and the other side of a node above the jump.

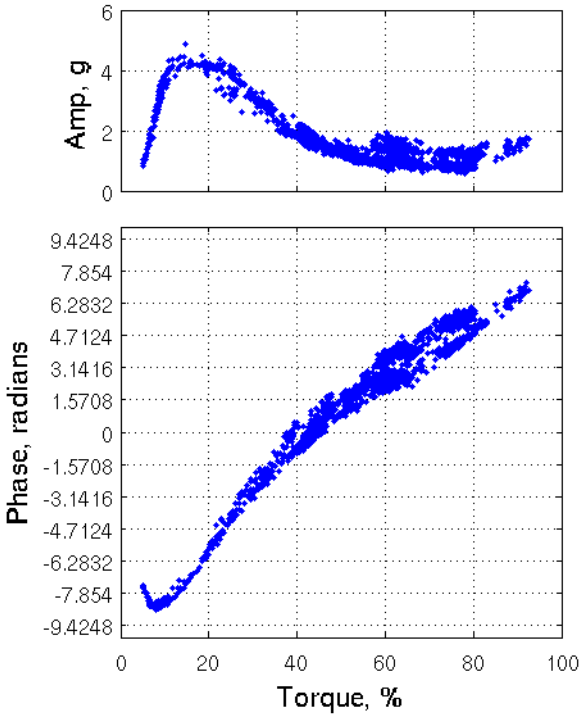

Figure 9 Measures of Bevel First Gear Mesh Harmonic for Accelerator 1, Flight 2.

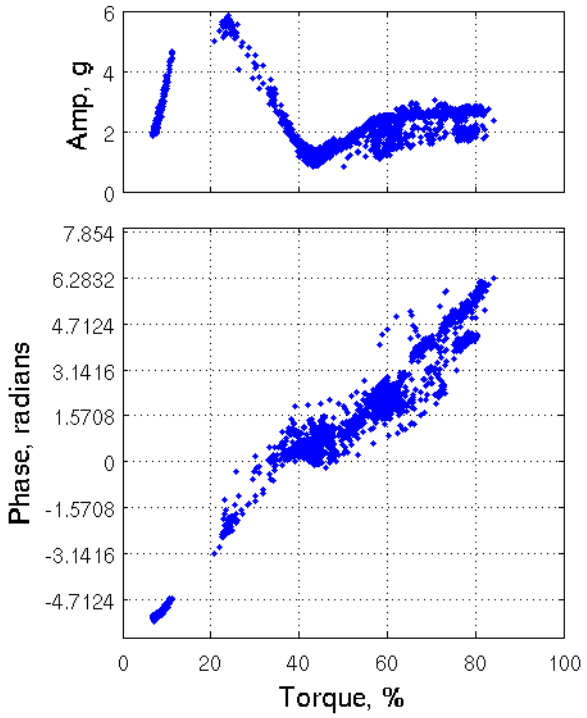

Figure 10 Measures of Bevel First Gear Mesh Harmonic for Accelerator 3, Flight 3.

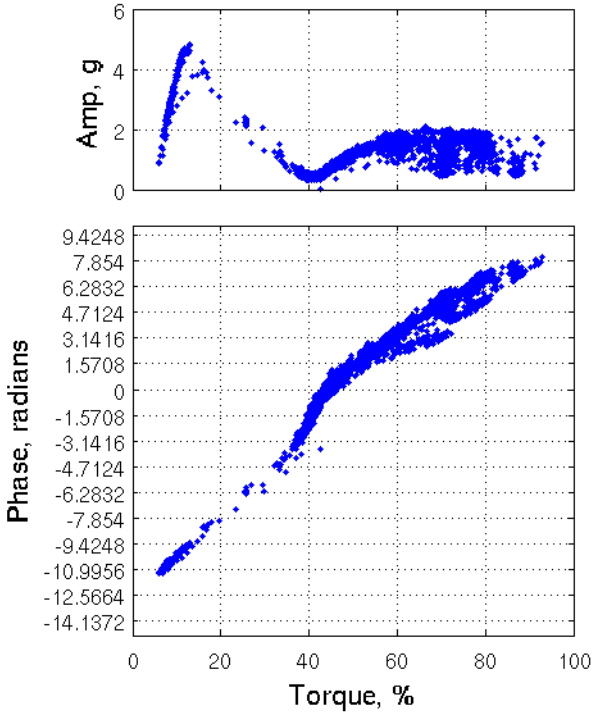

Figure 11 Measures of Bevel First Gear Mesh Harmonic for Accelerator 4, Flight 1.

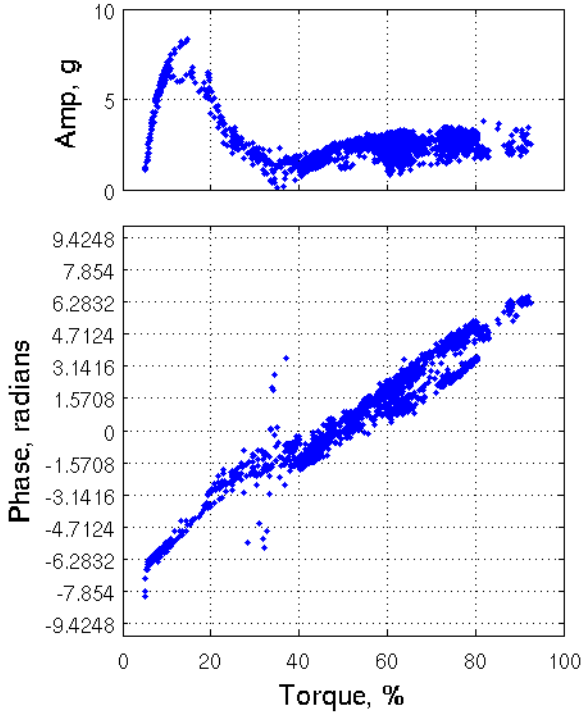

Figure 12 Measures of Bevel First Gear Mesh Harmonic for Accelerator 5, Flight 2.

A larger range of values of the phase and amplitude of both the planetary first gear mesh component and bevel gear mesh frequency exists over the range of about 50 to 80% torque. Also, the data over this torque range looks like it could be split into two separate groups. To investigate these observations, some cluster analyses were done on the phase data. Over limited torque ranges, the phase was fit to a linear curve, and two clusters were fit to the residuals by the k-means clustering method [15]. The amplitude and phase were then both viewed as functions of torque, RPM, ROC and speed for the two clusters. The clusters were found to belong to two very different fight regimes, one with the helicopter in climb at a lower ground speed with lower RPM, and the other with the helicopter in level flight at a higher ground speed with higher RPM. Figure 13 shows the two clusters for one example.

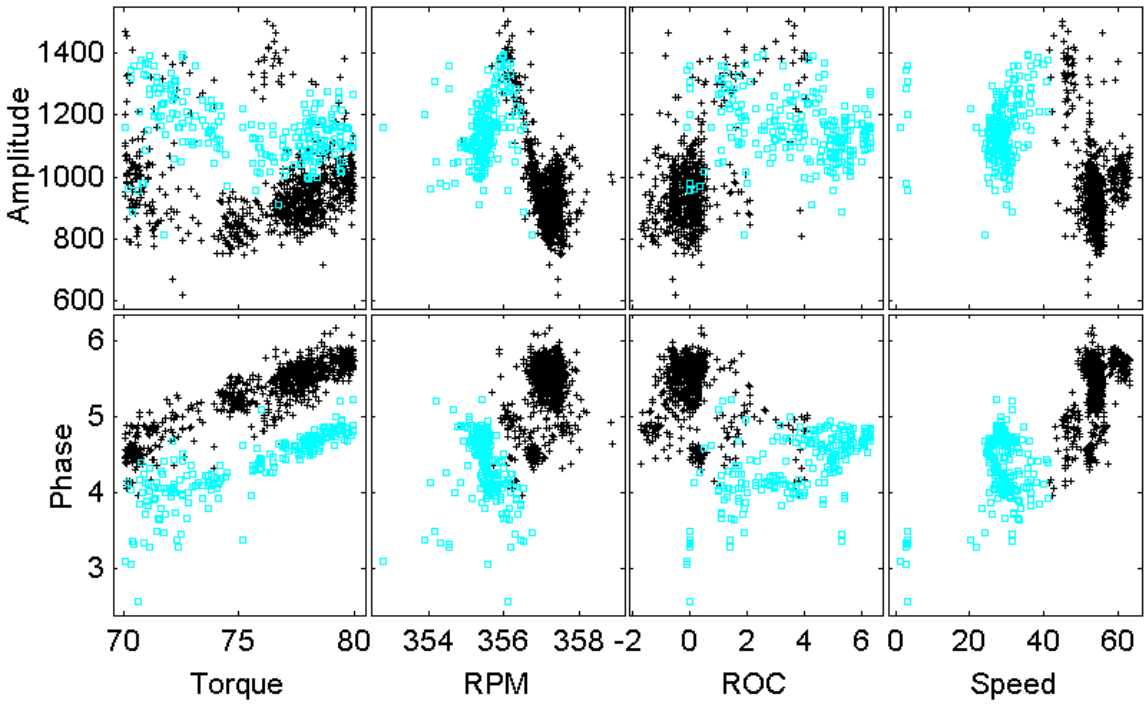

Figure 13 Cluster Analysis for Flight 1 Accelerometer 1, dark + = level flight, light square = climb at lower speed.

DISCUSION

Summary of Findings

1. The amplitude and phase of the first gear mesh components of both the planetary gear system and bevel gear display strong functional dependence on the torque.

2. Regarding amplitude of first gear mesh component:

   a. Amplitude of the first gear mesh component of the planetary gear system displays very high linear dependence on torque, increasing as torque increases.

   b. Amplitude of the bevel gear mesh frequency shows highly nonlinear functional dependence upon torque with a local maximum and minimum in the torque range. The location, steepness and depth of the local minima vary with accelerometer.

3. Regarding phase of first gear mesh component:

   a. Phase of the first gear mesh component of the planetary gear system displays very high linear dependence on torque, increasing as torque increases.

   b. Phase of the bevel gear mesh frequency contains a strong linear component dependant upon torque. Measurements on five of the six accelerometers also contain a nonlinear component to the phase

Presented at the American Helicopter Society 60th Annual Forum, Baltimore, MD, June 7-10, 2004.

variation with torque. This nonlinear component is either a section with a steeper slope or a section with flat slope and wider range. The location of the nonlinear component coincides with the local minima in the amplitude of the bevel gear mesh frequency.

4. Wider ranges in the phase and amplitude values were observed in the torque range of about 45% to 80%. The wider range was split with a cluster analysis into a region of level flight and another region of climb at lower speed.

Implications of Findings to HUMS

The signal shape variations found in this study have relevance to the construction of time synchronous averages, the interpretation of gear fault detection metrics and to the development and refinement of fault detection in flight. In order for time synchronous averaged data to properly represent the vibrations of the gear under consideration, the phases of the signals being averaged (time shifts in the signals) must be limited to reduce cancellation of the signal components by the averaging process. For example, if two signals of the same amplitude and a phase shift of π radians are averaged together, they will exactly cancel out each other. In order to minimize the phase range of signals when constructing an average, limits must be placed on the torque range and the flight condition, and flight state regions of wide phase variation and low amplitude must be avoided. The torque range limit depends upon the slope of the phase, which differed for the two gear systems.

Elaboration of Proposed Phase Jumping Explanation

In any dynamic, force driven system that supports wave propagation, a dynamic force applied at one location produces different responses at different locations. The response to the dynamic force at one location is the sum of the direct propagation of a wave plus all of the reflected waves. In the case of structures, such as this transmission, which support multiple types of wave propagation, there will be more than one direct wave. The multiple, discrete frequency waves propagating through the structure will form interference patterns that depend upon the frequency, stress tensor decomposition and location of the driving force, the shape of the structure and all of the boundary conditions on the structure. The interference pattern contains local maxima and minima. The more wavelengths that fit inside the structure, the more complicated the interference pattern becomes. Any changes in the frequency, force location, stress tensor decomposition, or boundary conditions result in changing the interference pattern. At some locations in the interference pattern, called nodes, there is zero response. The response on one side of a node is π radians out of phase with the response on the other side. The proposed explanation for the jumps in phase is that in one flight state the accelerometer is on one side of a node and in a different flight state the accelerometer is on the other side of the node due to changes in the interference pattern.

Dynamic Response at Accelerometer

The transfer functions measured in the tap test are an indication of how the accelerometers mounted on the transmission will modify the signal. The measured transfer function is not the transfer function from the gear vibration source to the accelerometer, so it is not appropriate to use measurements from the tap test to correct the measured vibration signal. The utility of the tap test is to estimate the extent of the effect of the transducer mounting to the signal. The resonances found in the tap test, indicate the vibration signal will be amplified at some frequencies due to the accelerometer mount.

Also, if the connection between the accelerometer mount and the transmission changes, the change needs to be considered in fault detection schemes. The strong vibration could loosen the connection between the accelerometer and transmission, thus moving resonances and changing the transfer characteristics to the transducer.

Flight State Space

The parameters describing the flight state space are limited to those available in this helicopter configuration. The inclusion of other parameters is desirable. We know from previous investigation [5] that sideways flight produces a marked change in the vibration signal, so aircraft based direction and angular measurements are desirable. It is highly likely that the turbulence induced vibration of the helicopter influenced the measured transmission vibration, so a turbulence measurement is also desirable.

CONCLUSIONS AND FUTURE RESEARCH

In flight vibration measurements from an OH-58C transmission were studied. Changes in the basic shape of the vibration were studied by a detailed examination

of the amplitude and phase of the first gear mesh components of the planetary gear system and bevel gear. Findings are listed below:

1) The amplitude and phase of the first gear mesh components of both the planetary gear system and bevel gear display strong functional dependence on the torque.

2) The phase variation in the signal must be considered when making time synchronous averages. Torque must be limited and the flight state limited to ensure a narrow phase range. The specific limitations will depend upon the gear and the transmission. Some flight regions will need to be avoided for some gears.

3) The linear component of the phase variation with torque is most likely due to strain in the shaft(s) connecting the gear to the timing signal.

4) Nonlinear components to the phase variation containing wider phase variation and/or range with torque could be due to interference effects in the propagation of the vibration from the source to the accelerometer. Multiple waves may occur due to multiple wave types (compressing and shear) and/or direct plus reflected waves.

Current plans include adding inertial measurements to the OH-58C and working with an UH-60L. The next step in studying the changes in the basic shape of the vibration is to examine their effect on gear fault metrics.

ACKNOWLEDGEMENTS

The authors would like to thank the Management of NASA's Computing, Information, and Communications Technology (CICT) Program, for providing the ongoing support for this effort. We would also like to complement the Army Flight Projects Office (FPO), headed by Major David Arterburn for the coordination of all aircraft instrumentation and operations. Thanks are extended to Mr. Munro Dearing, III, and Major David Arterburn who piloted the aircraft through daunting hours of flight tests. The authors would like to express gratitude to Mr. Larry Cochrane, Sigpro, for highly professional aircraft instrumentation and data collection support. Mr. Benton Lau performed the tap test and analysis.

REFERENCES

[1] Pourandier, J.-M. and Trouve, M., "An Assessment of European Experience in HUMS Development and Support," presented at 57th Annual Forum of the American Helicopter Society, Washington D.C., 2001.

[2] Keller, J. A. and Grabill, P., "Vibration Monitoring of UH-60A Main Transmission Planetary Carrier Fault," presented at 59th Annual Forum of the American Helicopter Society, Phoenix, AZ, 2003.

[3] Huff, E. M., Barszcz, E., Tumer, I. Y., Dzwonczk, M., and McNames, J., "Experimental analysis of Steady-State Maneuvering Effects on Transmission Vibration Patterns Recorded in an AH-1 Cobra Helicopter," in *56th Annual Forum*. Virginia Beach, VA: American Helicopter Society, 2000.

[4] Huff, E. M., Tumer, I. Y., and Mosher, M., "An Experimental Comparison of Transmission Vibration Responses from OH-58 and AH-1 Helicopters," presented at American Helicopter Society 57th Annual Forum, Washington D.C., 2001.

[5] Tumer, I. Y. and Huff, E. M., "Using Triaxial Accelerometer Data for Vibration Monitoring of Helicopter Gearboxes," presented at ASME Design Engineering Technical Conferences, Pittsburgh, PA, 2001.

[6] Mosher, M., Pryor, A. H., and Huff, E. M., "Evaluation of Standard Gear Metrics in Helicopter Flight Operation," presented at 56th Meeting of the Society for Machinery Failure Prevention Technology, Virginia Beach, VA, 2002.

[7] Huff, E. M., Mosher, M., and Barszcz, E., "An Exploration of Discontinuous Time Synchronous Averaging Using Helicopter Flight Vibration Data," presented at American Helicopter Society 59th Annual Forum,, Phoenix, AZ, 2003.

[8] Dempsey, P. J., Mosher, M., and Huff, E. M., "Threshold Assessment of Gear Diagnostic Tools on Flight and Test Rig Data," presented at American Helicopter Society 59th Annual Forum, Phoenix, AZ, 2003.

[9] Choy, F. K., Huang, S., Zakrajsek, J. J., Handschuh, R. F., and Townsend, D. P., "Vibration signature Analysis of a Faulted Gear Transmission System," in *30th Joint Propulsion Conference*. Indianapolis, Indiana: AIAA, 1994.

[10] Decker, H. and Lewicki, D. G., "Spiral Bevel Pinion Crack Detection in a Helicpoter Gearbox," presented at 59th Annual Forum of the American Helicopter Society, Phoenix, AZ, 2003.

[11] Barszcz, E., Huff, E. M., and Mosher, M., "Health Watch-2 System Overview," presented at American Helicopter Society 60th Annual Forum, Baltimore. MD, 2004.

[12] McFadden, P. D., "A Technique for Calculating the Time Domain Averages of the Vibration of the Individual Planet Gears and the Sun Gear in an Epicyclic Gearbox," *Journal of Sound and vibration*, vol. 144, pp. 163-172, 1991.

[13] McFadden, P. D., "Window Functions for the Calculation of the Time Domain Averages of the Vibration of the Individual Planet Gears and Sun Gear in an Epicyclc Gearbox," *Journal of Vibration and Acoustic*, vol. 116, pp. 179-187, 1994.

[14] Mosher, M., "A Simple Model for Understanding Vibration Measurements of Planetary Gear Systems," NASA Ames Research Center, NASA TM.

[15] Johnson, R. A. and Wichern, D. W., *Applied Multivariate Statistical Analysis*, 2 ed. Englewood Cliffs: Prentice-Hall, Inc., 1988.